

Supplementary Methods

CFSE cell proliferation

Excised spleen was smashed on 70 μm cell strainer. The RBCs in bone marrow and spleen were lysed with RBC lysis buffer (eBioscience). CD8^+ T cells were isolated from spleen by using a mouse CD8^+ T Cell Isolation Kit (Miltenyi Biotec) according to the manufacturer's instructions. gMDSCs were isolated from bone marrow of NSG mice and pre-metastatic livers of NSG mice bear tumors by Myeloid-Derived Suppressor Cell Isolation Kit (Miltenyi Biotec) according to the manufacturer's instructions. $\text{CD11b}^+\text{Ly6G}^{\text{high}}$ cells were eluted twice and the purity of $\text{CD11b}^+\text{Ly6G}^{\text{high}}$ cells is more than 95% (data not shown). CD8^+ T cells were labeled with 5 μM carboxyfluorescein succinimidyl ester (CFSE, Invitrogen, Grand Island, NY). CFSE-labeled CD8^+ T cells (1×10^6 /each well) and MDSCs were plated in a 24-well plate at ratios (T:MDSCs=1:0.125, 1:0.25, 1:0.5, or 1:1). CD8^+ T cells were activated by addition of 25 μl anti-CD3/CD28 mAb-coated beads (Dynabeads Mouse T-Activator CD3/CD28, Gibco) per well for 4 days. Controls included non-activated T cells and activated T cells with beads alone. T cell proliferation was measured by flow cytometry and the supernatants were subjected to ELISA.

Chemotaxis assay

CXCL1 was placed in the bottom chamber of a 24-well plate at a concentration of 1, 10, or 100 ng/ml. gMDSCs isolated from blood of NSG mice were seeded at a density of 1×10^6 /well in the upper chamber (3 μm , BD Falcon). For SB225002 treatment, gMDSCs isolated from blood of NSG mice were pre-treated with SB225002 at indicated doses for 1 h and then placed in the upper chambers. After incubation for 15 hr, migrated cells were counted by Vi-Cell™ XR (Beckman Coulter, Indianapolis, IN).

Cell viability assay

gMDSCs isolated from the pre-metastatic livers of NSG mice were seeded at a density of 3×10^5 /well (BD Falcon) and treated with CXCL1 at a concentration of 100 ng/ml for indicated days. The viable cells were counted by Vi-Cell™ XR.

Supplementary figures

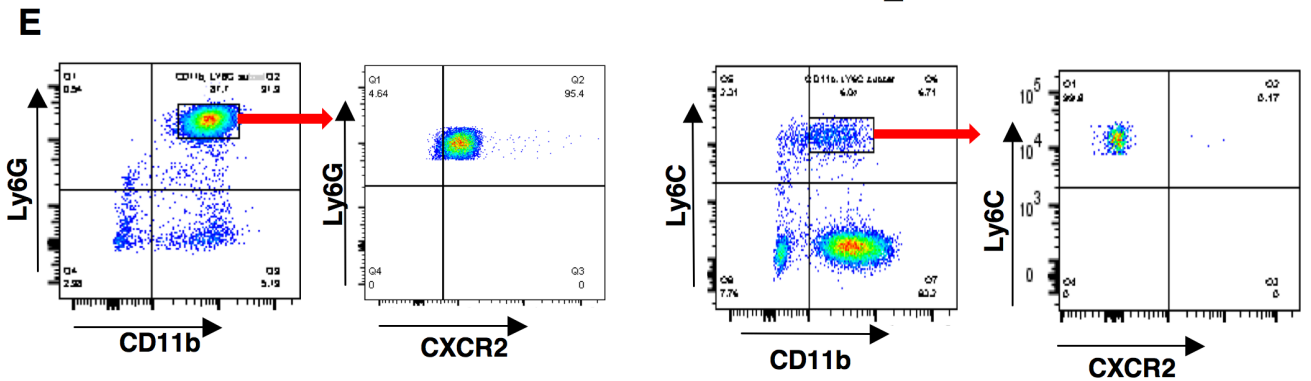
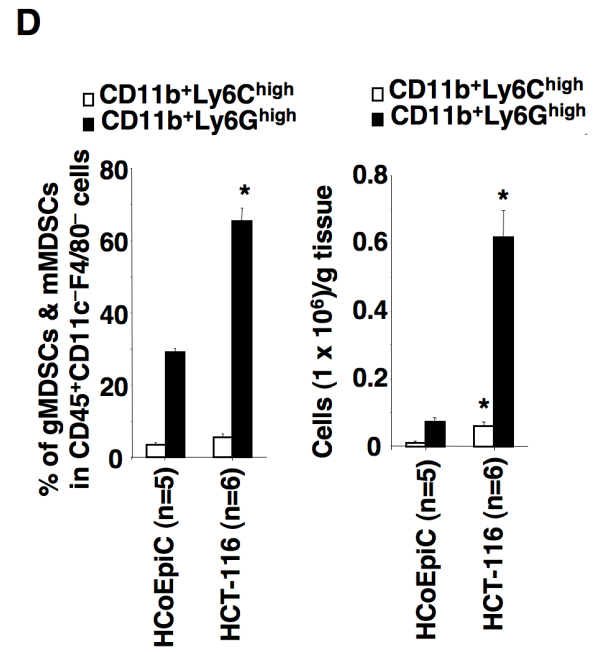
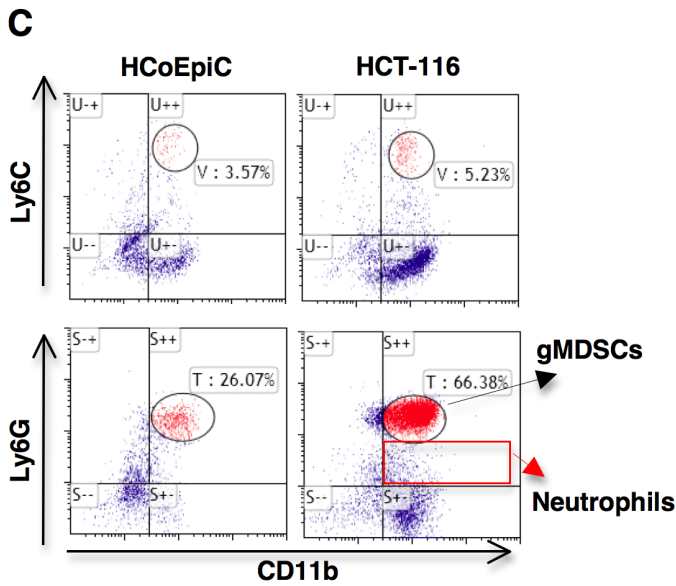
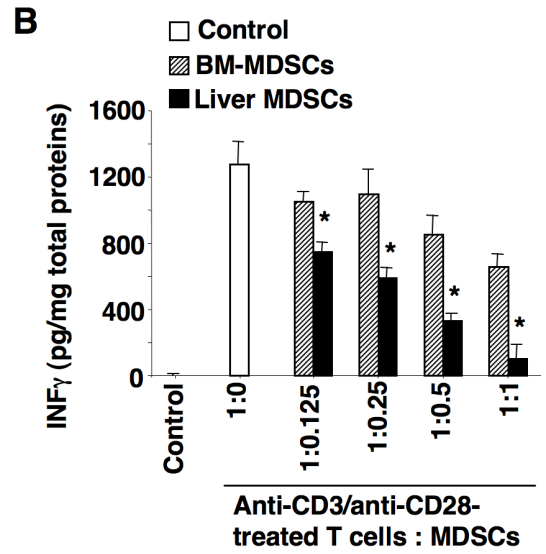
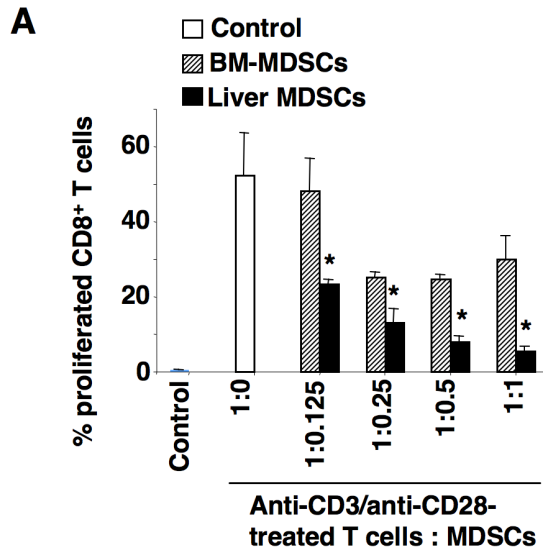


Figure S1. Granulocytic MDSCs in pre-metastatic livers

(A) The percentage of proliferated CD8⁺ T cells after co-culture of activated CD8⁺ T cells isolated from spleen with gMDSCs isolated from bone marrow of NSG mice or from pre-metastatic livers of NSG mice bear HCT-116 tumors at indicated ratio. (B) The protein levels of INF γ in the supernatant of co-culture of activated CD8⁺ T cells and gMDSCs as described in panel A. (C) The subpopulation of gMDSCs (CD11b⁺Ly6G^{high}), mMDSCs (CD11b⁺Ly6C^{high}), and neutrophils in pre-metastatic livers of NSG mice injected with HCoEpiC cells or HCT-116 cells was presented as percentage of gated CD45⁺CD11⁻F4/80⁻ granulocytes/monocytes. (D) The percentage (left panel) and numbers (right panel) of gMDSCs and mMDSCs in pre-metastatic livers from NSG mice as described in panel C. (E) The percentage of CXCR2-expressing gMDSCs and mMDSCs in total circulatory gMDSCs and mMDSCs, respectively. The error bar indicates \pm SEM. *p<0.05.

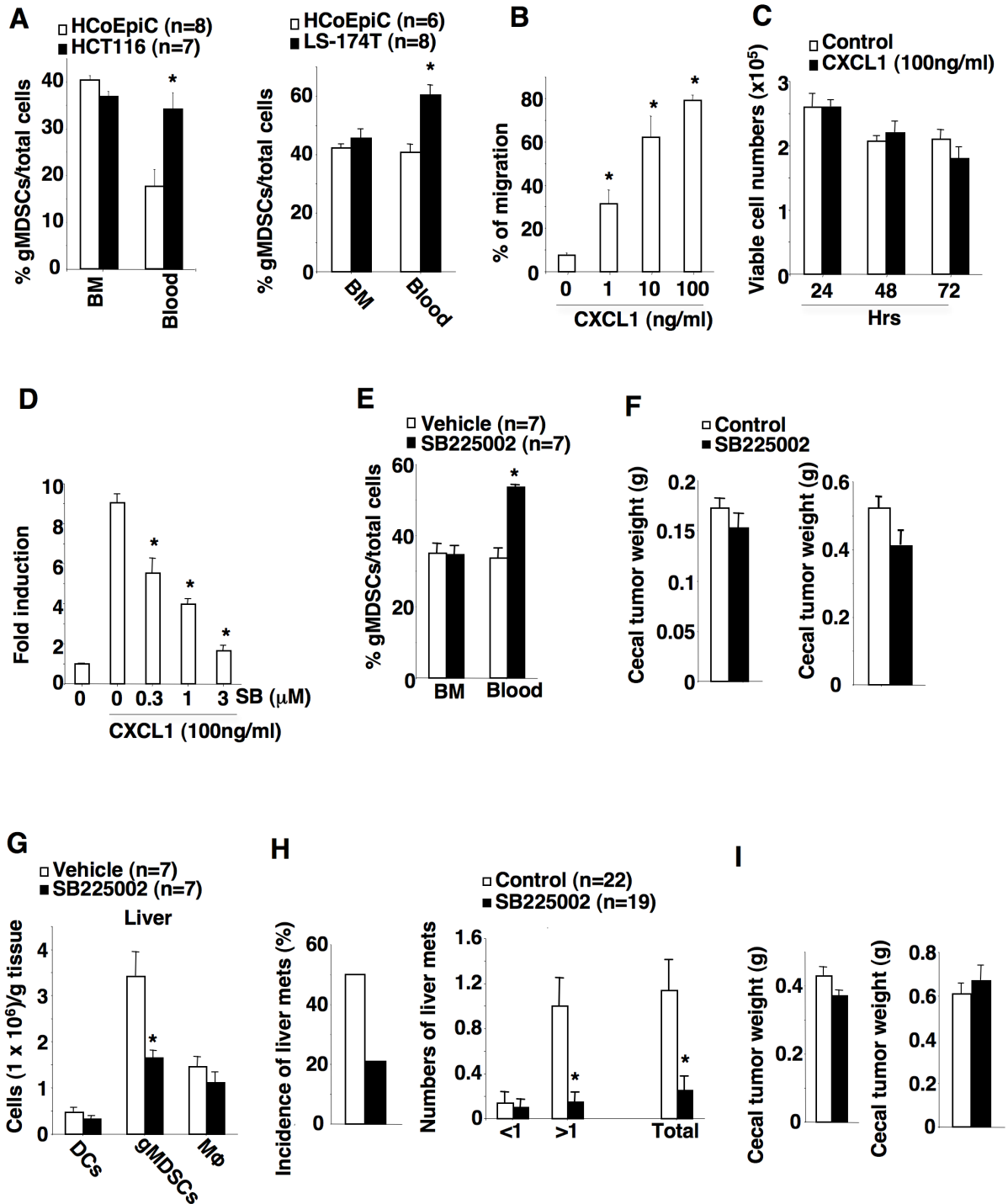


Figure S2. The CXCL1-CXCR2 axis is required for formation of pre-metastatic niches and liver metastasis

(A) Data represents the percentage of gMDSCs in total viable immune cells from bone marrow (BM) and peripheral blood taken from NSG mice injected with HCoEpiC cells, HCT-116 cells (left

panel), or LS-174T cells (right panel) as described in Fig. 2F. (B) CXCL1 induced chemotaxis in gMDSCs isolated from blood of NSG mice. (C) CXCL1 failed to induce expansion of gMDSCs isolated from pre-metastatic livers of NSG mice bearing tumors. (D) A CXCR2 antagonist, SB225002, inhibited CXCL1-induced chemotaxis in gMDSCs isolated from blood of NSG mice. (E) Data represents the percentage of gMDSCs in total viable immune cells from bone marrow (BM) and peripheral blood taken from NSG mice treated with vehicle or SB225002 after cecal injection of HCT-116 as described in Fig. 2G. (F) The weight of cecal tumor taken from mice without developing metastatic liver tumor (left panel) and with developing metastatic liver tumors (right panel) as described in Fig. 2G-H. (G) The numbers of DCs, gMDSCs, and macrophages in pre-metastatic livers of NSG mice treated with vehicle or SB225002 after cecal injection of LS-174T cells. (H) The incidence of liver metastasis (left panel) and the average numbers of liver metastatic tumors at different size and total that includes all sizes (right panel) in NSG mice treated with vehicle or SB225002 after cecal injection of LS-174T cells. (I) The weight of cecal tumor taken from mice without developing metastatic liver tumor (left panel) and with developing metastatic liver tumors (right panel) as described in panels G-H. The error bar indicates \pm SEM. * $p < 0.05$.

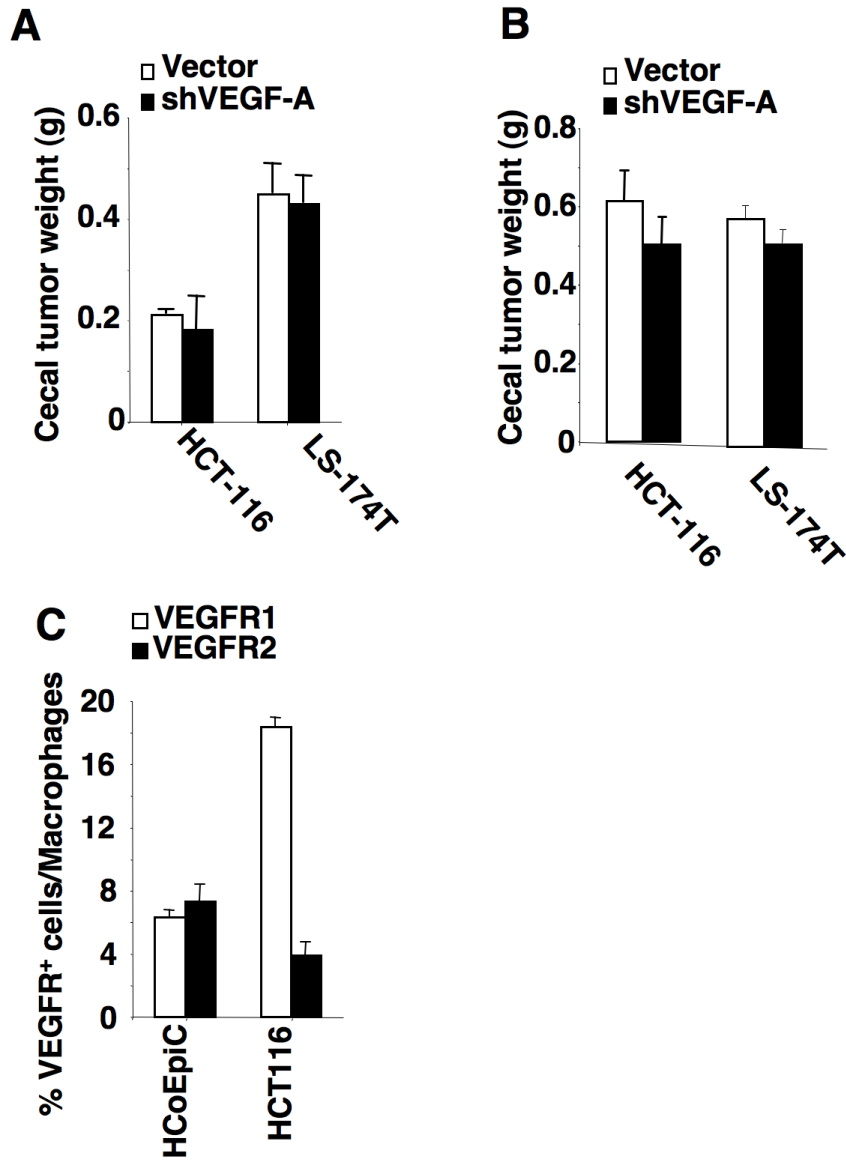


Figure S3. The effect of VEGF knockdown on cecal tumor growth and the VEGFR levels on the normal cecal macrophages and tumor-associated macrophages

(A-B) The weight of cecal tumor taken from mice without developing metastatic liver tumor (A) and with developing metastatic liver tumors (B) as described in Fig. 4B-D and Fig. 4E-F. (C) Data represents the percentage of VEGFR1- and VEGFR2-positive macrophages in total macrophages isolated from normal cecum injected with HCoEpiC cells and cecal tumors taken from NSG mice without developing metastasis after injection of HCT-116 cells.